Aerosol and Air Quality Research, 16: 2267–2277, 2016

ISSN: 1680-8584 print / 2071-1409 online
doi: 10.4209/aaqr.2016.01.0018

Adsorption/Desorption Behaviors of Acetone over Micro-/Mesoporous SBA-16 Silicas Prepared from Rice Husk Agricultural Waste

Wanting Zeng, Hsunling Bai*

Institute of Environmental Engineering, National Chiao Tung University, Hsinchu 300, Taiwan

ABSTRACT

The preparation of micro-/mesoporous SBA-16 adsorbent by rice husk derived sodium silicate as the silica source and its acetone adsorption/desorption behaviors were reported for the first time. The pore structural properties of waste-derived SBA-16 materials were controlled and optimized by adjusting the surfactant/silica molar ratios from 0.002 to 0.01 for achieving the best acetone adsorption performance. And the relationship between structural properties and acetone adsorption performances of SBA-16 adsorbents was investigated. The resultant waste-derived SBA-16 materials, denoted as RSBA-16, had specific surface areas of 575–1001 m^2 g^{-1}, pore sizes of 3.3–3.7 nm and pore volumes of 0.41–0.72 cm^3 g^{-1}. Among the studied adsorbents, RSBA-16(0.004) exhibited the highest saturated acetone adsorption capacity of 179 mg g^{-1}. It also showed excellent regeneration stability during 20 consecutive cycles. The results indicated that specific surface areas in both micro- and meso-pore ranges were the main factor that determined the superiority of acetone adsorption capacity of RSBA-16(0.004) over other adsorbents such as mesoporous RMCM-41 and micro-/mesoporous RSBA-15. The acetone adsorption experiments at 500–5000 ppmv demonstrated that the adsorption isotherm was well fitted with the Langmuir model, thus the adsorption of acetone on RSBA-16 might be a monolayer physisorption process. The results demonstrated the high adsorption capacity and cyclic stability of waste-derived RSBA-16(0.004) can be considered as a potential adsorbent for VOCs removals.

Keywords: VOCs adsorption; Rice husk; Adsorbents; Mesoporous cubic silica; Waste recovery.

INTRODUCTION

The control of volatile organic compounds (VOCs) emitted from industrial processes is an important issue because of their toxicity, odor and as O_3 precursors (Hseu *et al.*, 2013; Wu *et al.*, 2015). And adsorption is a popular VOCs control process due to its simple operation with efficient recovery of most VOCs (Jo and Chun, 2014; Bernabe *et al.*, 2015), with activated carbons (AC) as the most commonly employed VOCs adsorbents. However, the use of AC involves a number of problems such as its flammable property and regeneration difficulty (Fayaz *et al.*, 2015; Mohammed *et al.*, 2015; Niknaddaf *et al.*, 2016).

Ordered mesoporous silicas such as M41S and SBA-type materials have recently attracted enormous attention as alternative VOCs adsorbents because of their uniform and tailorable pore system as well as high specific surface area (Gibson, 2014). In this aspect, research studies on adsorptive removal of various VOCs over MCM-41, SBA-15, and MCM-48 have been reported (Serrano *et al.*, 2004; Dou *et al.*, 2011). Hung *et al.* (2009) investigated the adsorption behaviors of acetone vapors over MCM-41 and ZSM-5 zeolite. It was demonstrated that MCM-41 revealed better adsorption capability and regeneration ability in comparison to the ZSM-5 zeolite, an adsorbent used in commercialized zeolite rotor concentrators (Lin *et al.*, 2005).

More recently, research studies have shown that SBA-15 materials having dual micro-/mesopores are considered as better adsorbents in comparison to mesoporous MCM-41 (Kosuge *et al.*, 2007; Kubo and Kosuge, 2007). Zhang *et al.* (2012) conducted a comparative study on adsorption of toluene over MCM-41 and SBA-15. The results showed that SBA-15 exhibited superior adsorption capacities to those of MCM-41, which probably attributed to its two dimensional (2D) biporous (micro-/mesoporous) system. Similar observation was also reported recently by Liu *et al.* (2016), who demonstrated the favorable characteristic of micropores in SBA-15 materials for toluene adsorption.

The SBA-16 material has both micro- and mesopores with spheroidal mesopores connected by narrow entrances (Sakamoto *et al.*, 2000; Hwang *et al.*, 2004). Unlike MCM-41 and SBA-15 which have 2D hexagonal arrangement of uniform cylindrical mesopores, SBA-16 has a 3D cubic and cage-like pore system that provides more favorable mass

* Corresponding author.
Tel.: +886-3-573-1868; Fax: +886-3-572-5958
E-mail address: hlbai@mail.nctu.edu.tw

transfer of molecules within the pore channels (Rivera-Muñoz and Huirache-Acuña, 2010; Li *et al.*, 2016). Moreover, there are also a large number of micropores across the silica walls in SBA-16 (Van Der Voort *et al.*, 2002). These unique properties together with its good thermal stability of the thick wall and economical synthesis with inexpensive pore templates may make SBA-16 an attractive adsorbent for the environmental protection applications (Wei *et al.*, 2008; Chaudhuri *et al.*, 2016). Nevertheless, unlike the hexagonal form of SBA-15, the cubic form of SBA-16 mesoporous silica received much less attention. To the best of authors' knowledge, the research on adsorption of VOCs using SBA-16 made from either pure chemicals or waste resources has not been reported.

Using cheap and abundant silica sources instead of expensive ones is important to the production of silica based adsorbents at an industrial level (Chandrasekar *et al.*, 2008; Gérardin *et al.*, 2013). From this perspective, the recycling of silicon-rich solid wastes as alternative precursors will be highly practical and attractive (Ma and Ruan, 2013; Wang *et al.*, 2013; Kim *et al.*, 2015). In this work, SBA-16 materials are synthesized from the silica extracted from rice husk ash and applied for VOCs adsorption. Acetone is chosen as the representative compound because of its large usage in plastics, pharmaceutical, and semiconductor industries. The pore structure and BET characteristics of waste-derived SBA-16 materials were controlled and optimized by adjusting the surfactant/silica molar ratio for achieving the best adsorption performance of acetone, and the relationship between pore structure and adsorption performance was demonstrated. The performance of waste-derived SBA-16 adsorbents was also compared to that of SBA-16 made from pure chemical precursors as well as MCM-41, and SBA-15 manufactured by using rice husk derived sodium silicate as the silica precursors.

EXPERIMENTAL METHODS

Extraction of Silicate Supernatant

Rice husk ash (RHA) was obtained by heating rice husk at 400°C. The RHA was then mixed with aqueous 6M NaOH solution at 70°C for 12 h, and the resulting mixture was centrifuged to separate the silicate supernatant and sediment. The silicate supernatant was then utilized as the silica precursor for the synthesis of SBA-16 materials and named as RSBA-16 hereafter.

Synthesis of Adsorbents

The RSBA-16 material was synthesized using a tri-block copolymer, $EO_{106}PO_{70}EO_{106}$ (Pluronic F127, BASF) as the template and RHA-derived silicate solution as the silica source. The molar composition of the gel mixture was 1 SiO_2: 0.002–0.010 F127: 286 H_2O. For a typical synthesis, a given amount of F127 was dissolved in 20 g of DI water. Meanwhile, 82 mL of silicate solution was added to 70 mL of 6 M H_2SO_4 to achieve the pH value of 2. Subsequently, 6 M NaOH was added to the above silicate mixture to bring up the pH to 5 for accelerating the hydrolytic condensation reaction. After stirring, the surfactant solution was added slowly into the above mixture and the combined mixture was stirred for 15 min. The resulting gel mixture was transferred into a Teflon coated autoclave and kept in an oven at 100°C for 24 h. After cooling to room temperature, the resultant solid was recovered by filtration, washed with DI water and dried in an oven at 60°C for 24 h. Finally, the organic template was removed by using a muffle furnace in air at 500°C for 6 h. The RSBA-16 adsorbents synthesized from RHA at different Surf/Si molar ratios were named as RSBA-16(0.002), RSBA-16(0.004), RSBA-16(0.006), RSBA-16(0.008), and RSBA-16 (0.01).

For comparison purpose, the SBA-16 material was also prepared by using commercial chemical reagent of tetraethylorthosilicate (TEOS) as the silica precursor, and was denoted as SBA-16(TEOS). The molar composition of gel mixture was 1 SiO_2: 0.004 F127: 3 NaCl: 110 H_2O: 3.4 HCl. Detailed synthetic information for the synthesis of SBA-16(TEOS) can be referred to the literature (Wei *et al.*, 2008).

The synthesis of MCM-41 and SBA-15 from waste RHA was performed as well. The waste-derived MCM-41 was obtained by using RHA-derived silicate solution and cetyltrimethylammonium bromide (CTAB). The molar composition of the gel mixture was $1SiO_2$:0.2CTAB:$120H_2O$: $0.89H_2SO_4$. In a typical procedure, 89 mL of waste silicate solution was firstly acidified by adding approximately 40 mL of 2 M H_2SO_4 to bring down the pH to 10.5 with constant stirring to form a gel. After stirring, 7.28 g of CTAB (dissolved in 25 mL of DI water) was added drop by drop into the above mixture and the combined mixture was stirred for three additional hours. The resulting gel mixture was transferred into a Teflon coated autoclave and kept in an oven at 145°C for 36 h. After cooling to room temperature, the resultant solid was recovered by filtration, washed with DI water and dried in an oven at 110°C for 8 h. Finally, the organic template was removed in a muffle furnace (in air) at 550°C for 6 h.

The preparation of RHA-derived SBA-15 was similar to that of RSBA-16, except that EO_{20}-PO_{70}-EO_{20} (Pluronic P123, BASF) was used as the template. The organic P123 template was removed in a muffle furnace (in air) at 500°C for 6 h. The recycled MCM-41 and SBA-15 materials using RHA-derived silicate solution as the silica source was denoted as RMCM-41 and RSBA-15, respectively.

Characterization

The specific surface area and total pore volume of the samples were measured by nitrogen adsorption-desorption isotherms at –196°C using a surface area analyzer (Micromeritics, ASAP 2000). All the samples were degassed for 6 h at 300°C under vacuum (10^{-6} mbar) prior to the adsorption experiments. The specific surface areas of adsorbents were calculated by Brunauer-Emmett-Teller (BET) method in the relative pressure range P/P_0 = 0.05–0.3. The average pore sizes (D_p) of the adsorbents were determined by the Barrett-Joyner-Halenda (BJH) method, and their total pore volumes were obtained by the nitrogen amount adsorbed at P/Po = 0.99. The pore size distribution of MCM-41 was obtained from the analysis of the desorption branch of the isotherm by the BJH method, while nonlocal

density functional theory (NLDFT) method was used to determine the pore size distributions of both RSBA-15 and RSBA-16 samples (Liu *et al.*, 2016). The micropore size distributions of RSBA-15 and RSBA-16(0.004) were determined by the Horvath-Kawazoe model, and the micropore surface area and volume were calculated by the t-plot method.

The powder X-ray diffraction (XRD) analyses were made to reveal the crystalline structure of mesoporous materials, and the diffractograms of the mesoporous samples were recorded in the 2θ range of 0.5–4° in steps of 0.1 degree with a count time of 60 s at each point. Acetone temperature-programmed desorption (Acetone-TPD) was performed with an AutoChem II 2920 apparatus. Prior to the acetone-TPD experiments, the samples were preheated in air at 200°C for 2 h and cooled to 25°C. Then the samples were exposed to a flow of 500 ppmv acetone/He at 50°C for 1 h and then followed by argon purging for 1 h. Finally, the temperature was raised to 900°C in an Ar flow at a heating rate of 10 °C min^{-1}.

Acetone Adsorption Tests

Acetone adsorption experiments were performed with a lab-built packed column adsorber. The adsorbents were pelletized and sieved to size between 16–30 mesh (0.60–1.19 mm), and a total of 500 mg adsorbent was packed into an adsorption column with internal diameter of 0.7 cm. The adsorbents were pretreated before adsorption under nitrogen flow of 0.1 L min^{-1} at 200°C for 1 h. They were then cooled to 25°C for adsorption tests. Under a typical adsorption test, the acetone concentration was controlled at 1000 ppmv. But for obtaining the adsorption isotherm the concentrations of acetone were then varied in the range of 500–5000 ppmv. The packed column tests were performed with a total flow rate of 500 cm^3 min^{-1}. The concentration of acetone was continuously measured by a gas chromatograph (GC 7890, Agilent) equipped with a flame ionization detector (FID). The breakthrough time was defined at which the outlet concentration was about 10% of the inlet concentration. This corresponded to 90% acetone removal efficiency, and the acetone adsorption capacity at which is referred as the working capacity.

The Langmuir, Freundlich and Dubinin-Radushkevich equations were applied to study the acetone adsorption isotherms obtained at various inlet acetone concentrations. The Langmuir equation assumes monolayer adsorption onto a surface with a finite number of identical sits, and is represented as follows (Langmuir, 1916, 1918):

$$q_e = q_m K_a C_e / (1 + K_a C_e) \quad (1)$$

where C_e (ppmv) and q_e (mg g^{-1}) are the gas phase concentration and solid phase adsorption quantity of acetone at equilibrium, respectively; K_a is the Langmuir isotherm constant; q_m (mg g^{-1}) is the single layer acetone adsorption capacity.

The Freundlich equation is an empirical model that assumes the equilibrium adsorption capacity is linear with a change in adsorbate concentration on a log-log scale at a given temperature (Ruthven, 1984):

$$q_e = K_F C_e^{1/nf} \quad (2)$$

where C_e (ppmv) and q_e (mg g^{-1}) are the gas phase concentration and solid phase adsorption quantity of acetone at equilibrium; K_F is the Freundlich constant; and n_f is the heterogeneity factor.

The Dubinin-Radushkevich (DR) isotherm model is developed to determine the physisorption in microporous adsorbents, following a pore filling mechanism. The Dubinin-Radushkevich equation is as follows (Dubinin, 1989):

$$q_e = q_s \, exp\,(-K_{DR}\varepsilon^2) \quad (3)$$

$$\varepsilon = RTln(1 + 1/C_e) \quad (4)$$

where C_e (ppmv) and q_e (mg g^{-1}) are the gas phase concentration and solid phase adsorption quantity of acetone at equilibrium; q_s (mg g^{-1}) is the theoretical isotherm saturation capacity; K_{DR} (mol^2 kJ^{-2}) is a constant related to the mean free energy of adsorption; ε is the Dubinin-Radushkevich isotherm constant; R (J mol^{-1} K^{-1}) is the gas constant; and T (K) is the absolute temperature.

For understanding the stability of acetone adsorption/desorption process using the materials, a total of 20 adsorption/desorption cycles were performed in order to investigate the reversibility of acetone adsorption/desorption during the regeneration process. The adsorbents were activated by heating to 200°C for 1 h under a 0.1 L min^{-1} nitrogen flow. After cooling to 25°C, 1000 ppmv acetone was introduced until 90% acetone removal efficiency was reached. Subsequently, the acetone flow was then disconnected and the nitrogen flow at 0.1 L min^{-1} flow rate was introduced. The adsorbent was heated to 200 °C and kept constant for 30 min to desorb acetone from the adsorbent.

RESULTS AND DISCUSSION

Characterization of RSBA-16

Fig. 1 shows the powder XRD patterns of RSBA-16 samples prepared under various Surf/Si molar ratios. For the RSBA-16 samples, all of the XRD patterns showed one distinct diffraction reflection at 2θ value of 0.73–0.83°, which could be indexed as (1 1 0) reflection corresponding to a cubic Im3m structure (Hwang *et al.*, 2004; Wei *et al.*, 2008). It is found that the crystallinity of RSBA-16 samples was very sensitive to the Surf/Si molar ratio of the initial gel mixture. When the Surf/Si molar ratio of the initial gel was below 0.004 or above 0.008, one can see that crystallinity of RSBA-16 materials tended to decrease, suggesting the collapse of long range crystallographic order (Cheng *et al.*, 2003; Van Der Voort *et al.*, 2002). In addition, it is observed that the intensity of (1 1 0) reflection of RSBA-16(0.004) was similar to that of SBA-16(TEOS), which indicated the structural quality of RSBA-16(0.004) was as good as the SBA-16(TEOS) sample synthesized from TEOS. On the basis of the above results, it is therefore concluded that the excessive or insufficient surfactant concentration in the

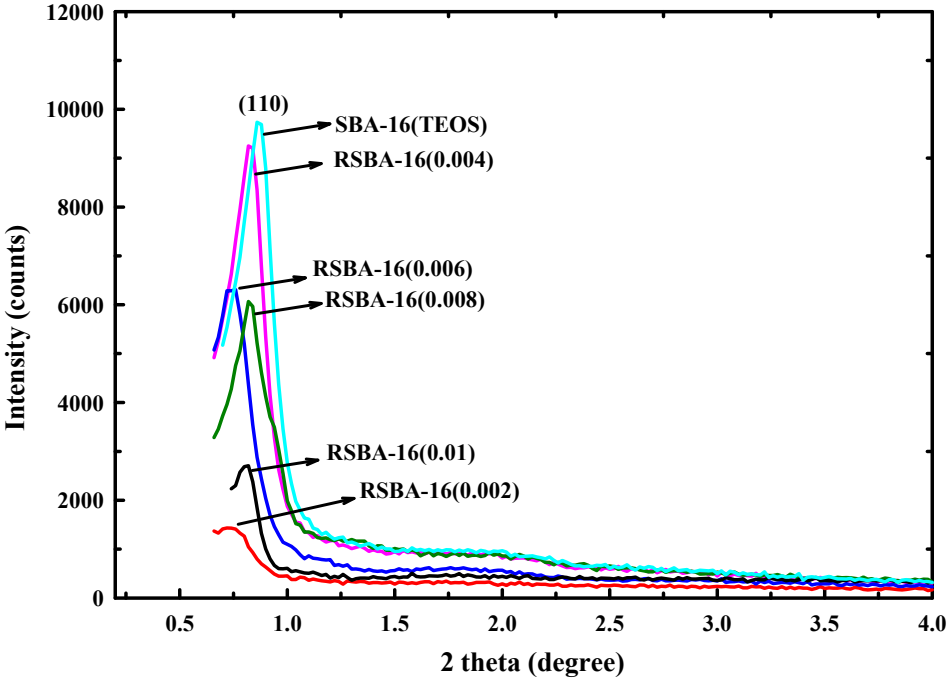

Fig. 1. Powder XRD patterns of RSBA-16 prepared at different Surf/Si molar ratios.

precursor mixture seemed unfavorable for establishing cubic architecture of RSBA-16.

The N_2 adsorption/desorption isotherms of all RSBA-16 samples are depicted in Fig. 2, where all samples displayed type IV isotherm of typical mesoporous materials according to the IUPAC classification, with a sharp capillary condensation step at intermediate P/Po of 0.4–0.6 (Zhao *et al.*, 1998). Furthermore, an obvious H2-typed hysteresis loop was observed for all RSBA-16 samples, which revealed the evidence of cage-like mesostructure with interconnectivity in a 3D pore system of SBA-16 materials (Gobin *et al.*, 2007). Also, it is noted that RSBA-16 samples showed a steep nitrogen uptake at very low relative pressure (P/Po = 0.02), which was related to the filling of micropores (Meynen *et al.*, 2009). The above results revealed that RSBA-16 samples exhibited a biporous system consisting of cubic mesopore channels that were connected by micropores (Kleitz *et al.*, 2003; Almeida *et al.*, 2012).

The BET specific surface area (S_{BET}), pore diameter (D_p) and total pore volume (V_{total}) of RSBA-16 are summarized in Table 1. It is observed both S_{BET} and V_{total} had maxima of 1001 m^2 g^{-1} and 0.72 cm^3 g^{-1} at a Surf/Si ratio of 0.004. And one can also see that the amount of micropores (V_{micro}) decreased continuously as a function of increasing Surf/Si ratio. It was reported that for the synthesis of SBA-16 materials at low Surf/Si ratios, microporous plugs were formed inside the 3D pore system which increased the amount of micropores in the system (Kim *et al.*, 2004). This is because that some of the triblock copolymers might not be involved in the actual templating of the mesopores, but still acted as templates for the formation of microporosity. Furthermore, it was noted that the surface area of RSBA-16(0.004) (1001 m^2 g^{-1}) was almost the same as that of SBA-16(TEOS) (1004 m^2 g^{-1}) prepared by using TEOS pure chemical as the silica precursor, revealing the high quality of the obtained RSBA-16(0.004).

Adsorption Performance of Acetone over RSBA-16

The breakthrough curves of 1000 ppmv acetone adsorption at 25°C over different RSBA-16 adsorbents are shown in Fig. 3. For comparison purpose, mesoporous material of RMCM-41 as well as micro-/mesoporous materials of RSBA-15 and SBA-16(TEOS) were also tested for their adsorption performance. And their structural properties are summarized in Table 1. One can see in Table 1 that these three materials have very high specific surface areas of over 1000 m^2 g^{-1}. But the RSBA-15 has a relatively low value of specific surface area in the micropore range (119 m^2 g^{-1}) as compared to those of the RSBA-16(0.004) (335 m^2 g^{-1}) and SBA-16(TEOS) (311 m^2 g^{-1}). Fig. 3 shows that all adsorbents had initial adsorption efficiencies of near 100%. And it is noticeable that the breakthrough time and the saturated time (C/C_o = 1.0) of the RSBA-16(0.004) were the longest among all tested adsorbents. This revealed that RSBA-16(0.004) had the highest acetone capacity among all tested adsorbents.

Table 1 summarizes the saturated acetone adsorption capacities of all adsorbents, and RSBA-16(0.004) has the highest acetone adsorption capacity of 179 mg g-adsorbent^{-1} among all tested adsorbents. To better understand the equilibrium acetone adsorption characteristics of RSBA-16 materials, the RSBA-16(0.004) sample was selected as the representative adsorbent because of its largest adsorption capacity. The experimental data were substituted into the Langmuir, Freundlich, and Dubinin-Radushkevich (D-R) isotherm models listed in Eqs. (1), (2) and (3), and the regression results are shown in Fig. 4. The equilibrium adsorption capacities (q_e) increased first and then remained

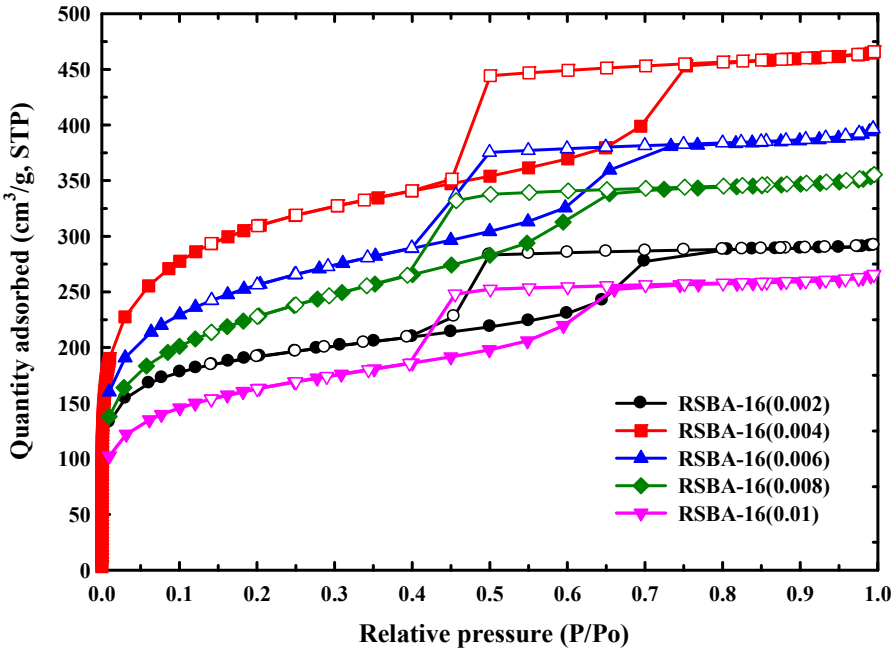

Fig. 2. Nitrogen adsorption-desorption isotherms of RSBA-16 prepared at different Surf/Si molar ratios.

Table 1. Structural parameters and adsorption performance of porous silica materials.

Sample name	Surf/Si molar ratio	[b]S_{BET} (m^2 g^{-1})	[c]S_{micro} (m^2 g^{-1})	[d]D_p (nm)	[e]V_{total} (cm^3 g^{-1})	[f]V_{micro} (cm^3 g^{-1})	Acetone capacity (mg g^{-1})		[g]Relative price of chemicals
							Saturated capacity (q_e)	Working capacity at 90% removal	
[a]RSBA-16(0.002)	0.002	663	386	3.7	0.45	0.175	116	68	-
RSBA-16(0.004)	0.004	1001	335	3.5	0.72	0.185	179	152	1.00
RSBA-16(0.006)	0.006	902	375	3.4	0.60	0.164	176	144	-
RSBA-16(0.008)	0.008	809	245	3.3	0.54	0.115	155	116	-
RSBA-16(0.01)	0.01	575	226	3.4	0.41	0.099	96	77	-
SBA-16(TEOS)	0.004	1004	311	3.9	0.78	0.190	180	152	1.52
RMCM-41	0.18	1064	-	3.3	1.00	-	108	79	3.70
RSBA-15	0.01	1009	119	4.3	0.93	0.04	144	116	0.93

[a] Sample name with "R" indicated that the material was prepared using rice husk derived precursor.
[b] BET surface area.
[c] Micropore surface area.
[d] Average pore diameter calculated by BJH theory.
[e] Total pore volume.
[f] T-plot micropore volume.
[g] The relative prices of chemicals were calculated based on the ratios of the purchase price of chemicals used for manufacturing the adsorbents to that for the manufacture of RSBA-16(0.004).

almost the same when further increasing the acetone concentration (C_e). The calculated correlation coefficients (R^2) between these isotherm equations and experimental data were 0.999, 0.850 and 0.937, respectively, for Langmuir, Freundlich and D-R isotherm models. These observations infer that monolayer physisorption could be the main process since the Langmuir adsorption isotherm model showed the best agreement with the experimental data.

It is clear from Fig. 4 that Langmuir equation is the best isotherm model to describe the experimental observation. The Langmuir model assumes monolayer coverage of adsorbate on the surface of adsorbent, thus it is expected that the acetone adsorption capacity should be linearly correlated to the specific surface area of the adsorbent. This is demonstrated by Fig. 5 for the linear increase of acetone adsorption capacity with the increase of specific surface area. The linear regression coefficient (R^2) between the acetone adsorption capacity and the specific surface area of RSBA-16 adsorbents was 0.96. A similar observation has been found over SBA-15 materials for the adsorption of naphthalene (Liu *et al.*, 2016).

As can be seen in Table 1, the acetone capacity of RSBA-16(0.004) was similar to that of SBA-16(TEOS) made from commercial chemicals. This is expected since they

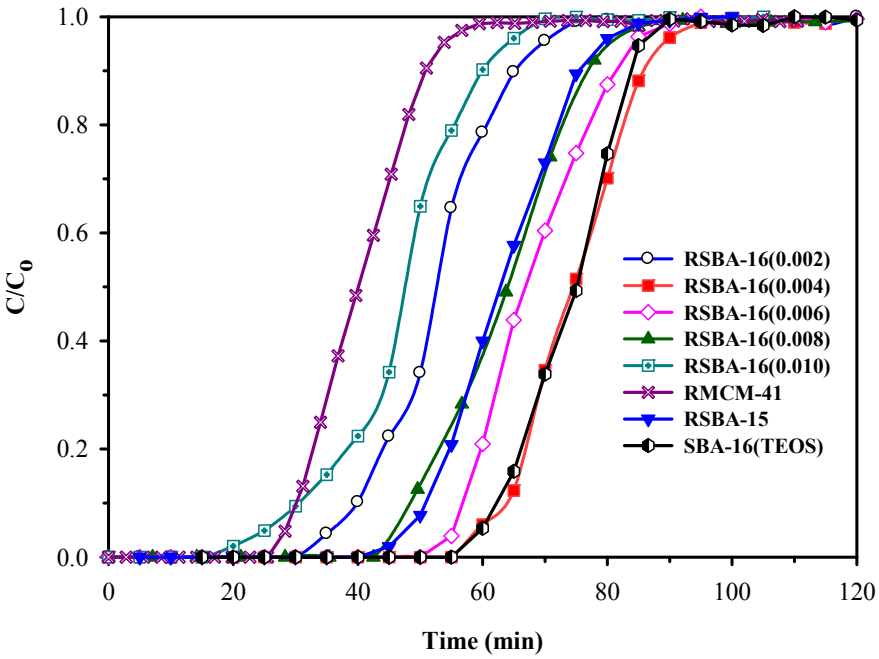

Fig. 3. Acetone breakthrough curves of various adsorbents tested with 1000 ppmv acetone at 25°C.

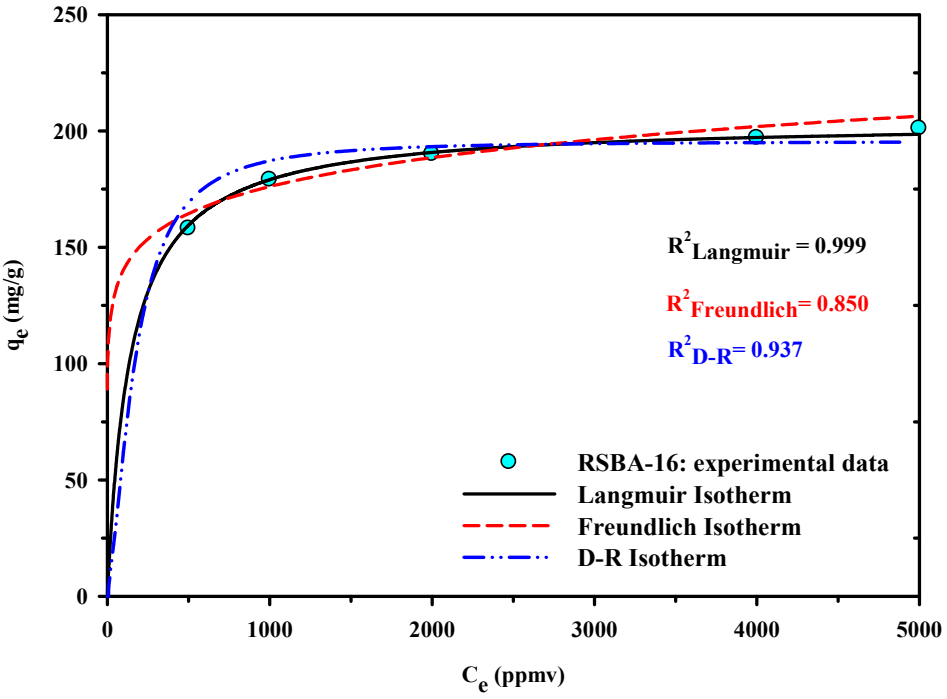

Fig. 4. Langmuir, Freundlich and Dubinin-Radushkevich adsorption isotherms for RSBA-16(0.004) adsorbent.

both had very similar pore textural properties. In addition, although these three materials of RSBA-16(0.004), RMCM-41 and RSBA-15 had similar specific surface areas of around 1000 m^2 g^{-1}, the adsorbent of RSBA-16(0.004) showed a better adsorption capacity than the other two adsorbents. This might be due to that the presence of micropores in the mesoporous silica materials is beneficial for enhancing the adsorption performances of VOCs. The pore size closed to the molecular size of gaseous molecules might have a molecular sieving effect, which acted as a trap for retaining the gaseous molecules within the pores (Kosuge *et al.*, 2007; Zhang *et al.*, 2012).

Fig. 6(a) depicts the micropore size distributions of RSBA-15 and RSBA-16(0.004). Both samples showed similar micropore size distribution in the range of 0.4–0.9 nm with a mode peak at ca. 0.55 nm, which was close to the molecular size of acetone (0.43 nm). And RSBA-16(0.004) exhibited a higher peak intensity (dV/dD) on this micropore range than

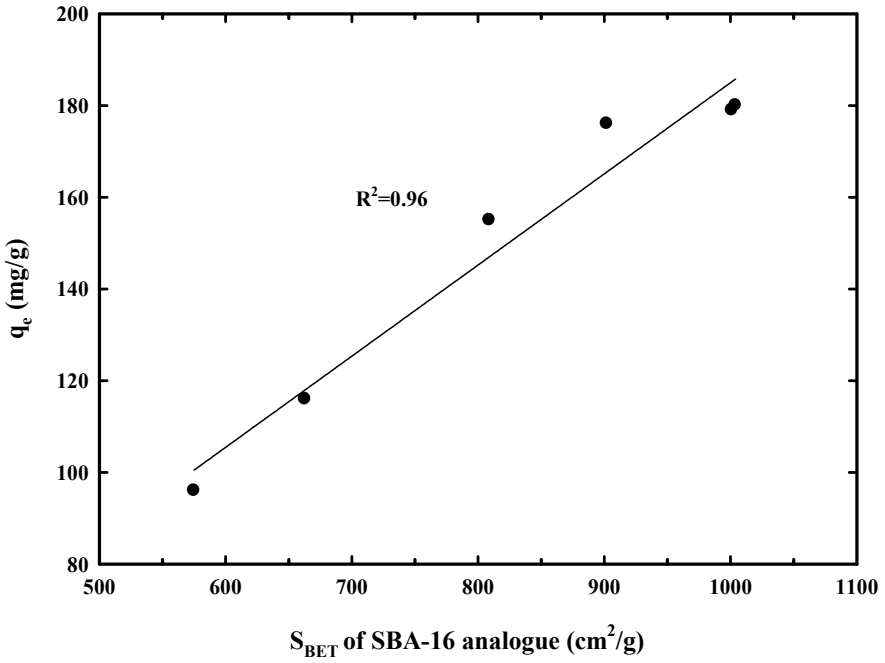

Fig. 5. Correlation between the specific surface areas of RSBA-16 adsorbents and their acetone adsorption capacities. Adsorption temperature: 25°C; Acetone inlet concentration: 1000 ppmv.

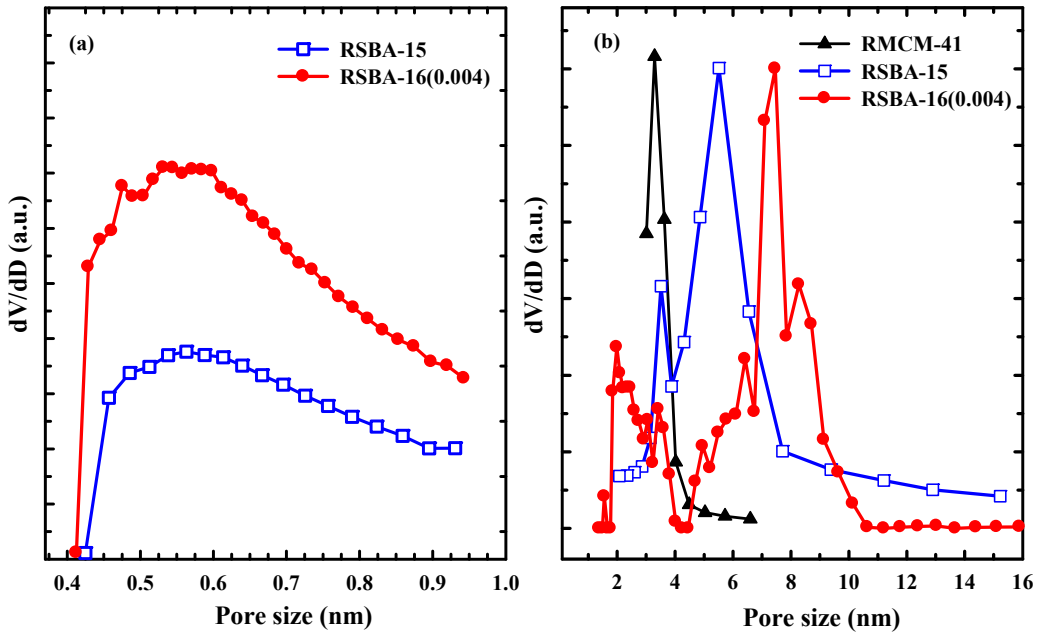

Fig. 6. (a) Micropore size distribution of RSBA-15 and RSBA-16(0.004); and (b) Mesopore size distributions for RMCM-41, RSBA-15, and RSBA-16(0.004).

that of the RSBA-15. Furthermore, Fig. 6(b) showed that RSBA-16(0.004) also displayed a higher peak intensity on small mesopores ($D_p < 3$ nm). The observations from Figs. 6(a) and Fig. 6(b) are consistent with the higher value of micropore surface area of RSBA-16(0.004) than that of RSBA-15 as shown in Table 1. This also helps to explain that the observed monolayer adsorption in Figs. 4 and 5 since RSBA-16 adsorbent has a significant portion in micropore and small mesopore ranges. This is also the main reason for the superior adsorption performance of RSBA-16(0.004) as compared to that of the RMCM-41 which has only mesopores. Accordingly, one may conclude that specific surface areas in both micro- and meso-pore ranges were the main factor that determined the superiority of acetone adsorption capacity of RSBA-16(0.004) adsorbent over other adsorbents such as mesoporous RMCM-41 and micro-/mesoporous RSBA-15.

For the practical application, the adsorbent is replaced or

regenerated at the break point to maintain the designed removal efficiency (e.g., 90% removal). One can see in Table 1 that the break point (at 90% acetone removal efficiency) adsorption capacity of RSBA-16(0.004) sample was 152 mg g^{-1}. This was much higher than those of RMCM-41 (79 mg/g) and RSBA-15 (116 mg g^{-1}) under the same conditions.

Table 2 compares the acetone adsorption capacities of this study with others available in the literature. It is observed that the RSBA-16(0.004) developed in this study had the highest acetone adsorption capacity among all adsorbents under comparable conditions except the coconut based activated carbon. The adsorption capacity of coconut-derived activated carbon (117 mg g^{-1} at 20°C, 200 ppmv inlet condition) had a similar adsorption capacity to that of RSBA-16(0.004) (115 mg g^{-1} at 25°C, 200 ppmv inlet condition). However, the flammable nature of the carbon-based sorbent might limit its potential use for cyclic VOCs adsorption-desorption applications.

Cyclic Acetone Adsorption/Desorption Tests

The acetone-TPD measurement was performed to understand the desorption behaviors of RSBA-16(0.004), RMCM-41, and RSBA-15 samples, with results shown in Fig. 7. It has been reported that the desorption performance of adsorbent is mainly associated with the interaction between adsorbent surface and adsorbate molecules (Zhang *et al.*, 2012). All mesoporous silica adsorbents showed a sharp desorption peak in the range of 100–200°C. Compared to RMCM-41 and RSBA-15 samples, the TPD profile of RSBA-16(0.004) showed a slight shift toward higher temperature, suggesting a stronger interaction between acetone molecules and RSBA-16(0.004). This observation could be due to the difference in the micro-/mesoporous structure between these three adsorbents as discussed previous by Fig. 6. The presence of micropores (0.4–0.9 nm) and relatively small mesopores (D_p < 3 nm) may result in strong interaction between the acetone molecule and the pore surface of RSBA-16(0.004).

Temperature swing adsorption (TSA) process has been widely adopted for the adsorptive gas separation in practical application (Gabruś *et al.*, 2015). As evidenced from the acetone-TPD results, most of acetone molecules can be effectively desorbed from the adsorbent surfaces of RMCM-41, RSBA-15 and RSBA-16(0.004) at 200°C. Therefore, the following cyclic adsorption/desorption tests were conducted using 200°C as the desorption temperature, and 25°C as the adsorption temperature. Fig. 8 displays the working capacity and adsorption index of RMCM-41, RSBA-15, and RSBA-16(0.004) during 20 cycles of adsorption/desorption operation. The adsorption index was calculated as the percentage ratio of the working capacities of the regenerated adsorbents to that of the fresh adsorbent, thus 100% adsorption index implies that the adsorbent was not deteriorated at all.

It can be seen in Fig. 8 that the acetone working capacity for RMCM-41, RSBA-15, and RSBA-16(0.004) decreased from 79, 116 and 152 mg g^{-1} for the fresh adsorbents to 75, 106 and 140 mg g^{-1}, respectively, for adsorbents after the first cycle of operation. Then the adsorption capacities were quite stable during the following 19 cycles of operation for all materials. The average adsorption indexes of RMCM-41, RSBA-15 and RSBA-16(0.004) adsorbents during the 20 regeneration cycles were 91.7 ± 2.4%, 91.4 ± 1.5% and 90.5 ± 1.3%, respectively. The insignificant difference on the cyclic adsorption/desorption performance over these three samples could be attributed to the intrinsic nature of acetone, which is a polar compound with small molecular size and high vapor pressure, making it to be easily desorbed from all three materials. As a result, RSBA-16(0.004) still retained the highest adsorption capacity of 137 mg g^{-1} as compared to those of RMCM-41 (72 mg g^{-1}) and RSBA-15 (106 mg g^{-1}) adsorbents after 20 cycles. This result indicates that RSBA-16(0.004) can be employed as a stable acetone adsorbent through cyclic TSA operation.

Besides having high adsorption performance and regeneration stability, the production cost is also one of the most important considerations for industrial applications. It

Table 2. Comparison of acetone adsorption capacity of various adsorbents tested by this study and literature.

Adsorbent	Saturated acetone capacity, q_e (mg g^{-1})	Temperature (°C)	Test concentration (ppmv)	Reference
RSBA-16(0.004)	115	25	200	This study
	179		1000	
	190		2000	
	201		5000	
AC	200	10	8800	Tang *et al.* (2016)
AC	184	25	2000	Li *et al.* (2012)
DAY-zeolite	137	20	2.27×10^5	Lee *et al.* (2011)
Mesoporous silica spherical particles	130	25	1000	Hung and Bai (2008)
H-ZSM-5	86	25	8700	Hung and Bai (2008)
Nanostructured zeolite particles	83	25	1000	Lin and Bai (2006)
Coconut based AC	117	20	200	Lee *et al.* (2006)
ACF	3.0	25	1000	Mangun *et al.* (1999)

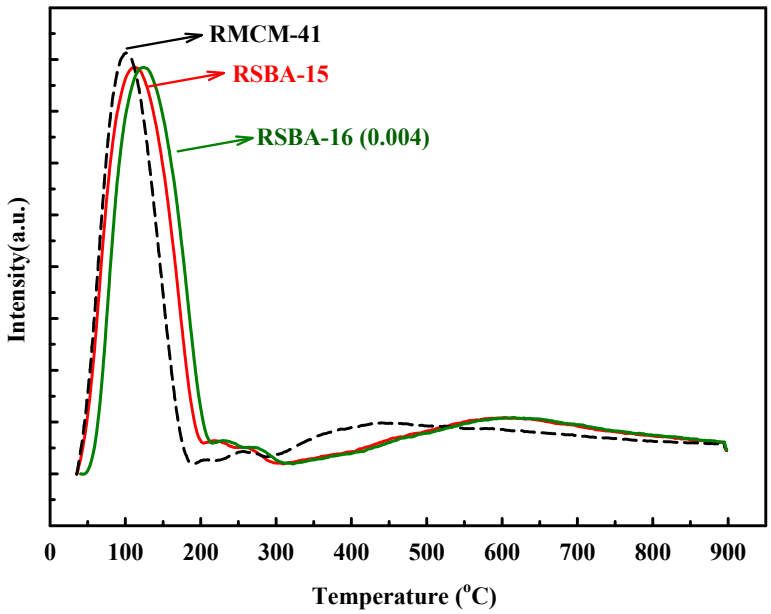

Fig. 7. Acetone-TPD plots of RSBA-16(0.004), RMCM-41, and RSBA-15 adsorbents.

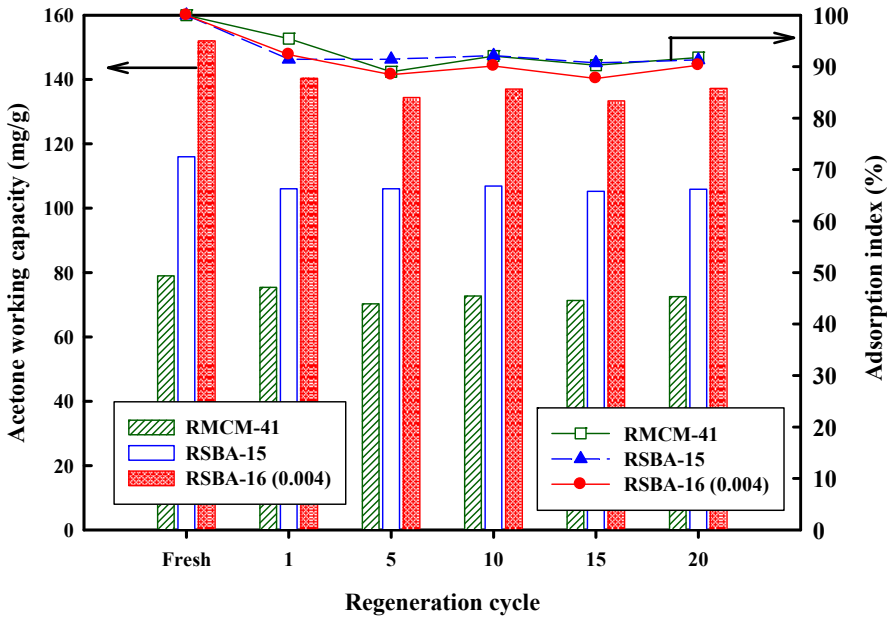

Fig. 8. Cyclic acetone adsorption/desorption performance (working capacity and adsorption index) with RSBA-16(0.004), RMCM-41, and RSBA-15 adsorbents. Cyclic condition: Adsorption temperature: 25°C; Acetone inlet concentration: 1000 ppmv; Desorption temp: 200°C, Desorption time: 30 min.

can be seen in Table 1 that the chemical cost of RSBA-16(0.004) is only two-third to that of SBA-16(TEOS). And when considering the need of treatment and disposal of rice husk waste, then the cost of RSBA-16 materials can be decreased further. On the other hand, even though the chemical cost of RSBA-16(0.004) is slightly higher than that of RSBA-15, the acetone adsorption capacity (179 mg g^{-1}) of RSBA-16(0.004) is much higher than that of RSBA-15 (144 mg g^{-1}). Therefore, for obtaining the same acetone adsorption capacity, the quantity of RSBA-16(0.004) adsorbent can be reduced in comparison with that of RSBA-15. This would provide a high advantage for practical adsorption application using RSBA-16(0.004) since it can reduce the adsorber volume of VOCs adsorption. And RSBA-16(0.004) also showed much lower chemical cost and much higher adsorption capacity than those of RMCM-41. Accordingly, RSBA-16(0.004) is a better adsorbent for VOCs removals owing to its superior adsorption capability and higher adsorption capacity/price value.

For the synthesis of SBA-16 materials, the use of the commercial silicate source (e.g., TEOS) accounts for a significant portion of the manufacturing cost, since the other

reagent (e.g., the structure directing template of F127) can be easily recycled using the solvent extraction approach under mild conditions (Jia *et al.*, 2013; Ng *et al.*, 2013). Therefore the use of rice husk agricultural waste instead of commercial silica source as a cheap and abundant silica precursor appears to be highly beneficial for synthesizing RSBA-16 materials at an industrial level.

CONCLUSIONS

In this work, the adsorption/desorption behaviors of acetone on SBA-16 adsorbents prepared by using silicate precursor from rice husk waste has been demonstrated for the first time. The results revealed that specific surface areas in both micro- and meso-pore ranges were the main parameter affecting the acetone adsorption performance of rice husk ash-derived SBA-16 adsorbents. And it was demonstrated that rice husk ash-derived SBA-16(0.004) had a very similar pore structure and acetone capacity to those of the SBA-16 made from pure chemicals. This reveals the high potential of using rice husk waste to manufacture SBA-16 material of the same quality as that made with pure chemicals. Compared to rice husk ash-derived MCM-41 and SBA-15 adsorbents, rice husk ash-derived SBA-16(0.004) showed important advantages of high adsorption capacity and good cyclic adsorption/desorption stability. Moreover, to adsorb the same quantity of acetone, the amount of rice husk ash-derived SBA-16(0.004) was also lower than that of rice husk ash-derived SBA-15. Consequently, less space was required when rice husk ash-derived SBA-16(0.004) was used as an adsorbent. Future work is needed to test on the adsorption of different adsorbates such as toluene and 1,2,4-trimethylbenzene (TMB) so that the properties and roles of SBA-16 micro-/mesoporous adsorbents can be further clarified when applied to the VOCs adsorption processes.

ACKNWOWLEDGEMENT

The authors gratefully acknowledge the financial support from the Ministry of Science and Technology of Taiwan, R.O.C. through grant No.: NSC 102-2221-E-009-009-MY3.

REFERENCES

Almeida, R.K.S., Pires, C.T.G.V.M.T. and Airoldi, C. (2012). The influence of secondary structure directing agents on the formation of mesoporous SBA-16 silicas. *Chem. Eng. J.* 203: 36–42.

Bernabe, D.P., Herrera, R.A.S., Doma, B.T., Fu, M.-L., Dong, Y.C. and Wang, Y.F. (2015). Adsorption of low concentration formaldehyde in air using ethylene-diamine-modified diatomaceous earth. *Aerosol Air Qual. Res.* 15: 1652–1661.

Chandrasekar, G., You, K.S., Ahn, J.W. and Ahn, W.S. (2008). Synthesis of hexagonal and cubic mesoporous silica using power plant bottom ash. *Microporous Mesoporous Mater*. 111: 455–462.

Chaudhuri, H., Dash, S., Ghorai, S., Pal, S. and Sarkar, A. (2016). SBA-16: Application for the removal of neutral, cationic, and anionic dyes from aqueous medium. *J. Environ. Chem. Eng.* 4: 157–166.

Dou, B., Hu, Q., Li, J., Qiao, S. and Hao, Z. (2011). Adsorption performance of VOCs in ordered mesoporous silicas with different pore structures and surface chemistry. *J. Hazard. Mater.* 186: 1615–1624.

Dubinin, M.M. (1989). Fundamentals of the theory of adsorption in micropores of carbon adsorbents: Characteristics of their adsorption properties and microporous structures. *Carbon* 27: 457–467.

Fayaz, M., Shariaty, P., Atkinson, J.D., Hashisho, Z., Phillips, J.H., Anderson, J.E. and Nichols, M. (2015). Using microwave heating to improve the desorption efficiency of high molecular weight VOC from beaded activated carbon. *Environ. Sci. Technol.* 49: 4536–4542.

Gabruś, E., Nastaj, J., Tabero, P. and Aleksandrzak, T. (2015). Experimental studies on 3A and 4A zeolite molecular sieves regeneration in TSA process: Aliphatic alcohols dewatering–water desorption. *Chem. Eng. J.* 259: 232–242.

Gérardin, C., Reboul, J., Bonne, M. and Lebeau, B. (2013). Ecodesign of ordered mesoporous silica materials. *Chem. Soc. Rev.* 42: 4217–4255.

Gibson, L.T. (2014). Mesosilica materials and organic pollutant adsorption: Part A removal from air. *Chem. Soc. Rev.* 43: 5163–5172.

Gobin, O.C., Wan, Y., Zhao, D., Kleitz, F. and Kaliaguine, S. (2007). Mesostructured silica SBA-16 with tailored intrawall porosity part 1: Synthesis and characterization. *J. Phys. Chem. C* 111: 3053–3058.

Hseu, Z.Y., His, H.C., Syu, J.S. and Wang, L.C. (2013). Development of porous template carbons from montmorillonite clays and evaluation of their toluene adsorption behaviors. *Aerosol Air Qual. Res.* 13: 1779–1789.

Hung, C., Bai, H. and Karthik, M. (2009). Ordered mesoporous silica particles and Si-MCM-41 for the adsorption of acetone: A comparative study. *Sep. Purif. Technol*. 64: 265–272.

Hung, C.T. and Bai, H. (2008). Adsorption behaviors of organic vapors using mesoporous silica particles made by evaporation induced self-assembly method. *Chem. Eng. Sci.* 63: 1997–2005.

Hwang, Y.K., Chang, J.S., Kwon, Y.U. and Park, S.E. (2004). Microwave synthesis of cubic mesoporous silica SBA-16. *Microporous Mesoporous Mater*. 68: 21–27.

Jia, D., Song, M., Ye, X., Gu, H., Zou, C., Niu, G. and Zhao, D. (2013). Recycling mother liquor to synthesize mesoporous SBA-15 silica. *Asian J. Chem.* 25: 9627–9631.

Jo, W.K. and Chun, H.H. (2014). Application of Fibrous activated carbon filter in continuous-flow unit for removal of volatile organic compounds under simulated indoor conditions. *Aerosol Air Qual. Res.* 14: 347–354.

Kim, S., Han, Y., Park, J. and Park, J. (2015). Adsorption characteristics of mesoporous silica SBA-15 synthesized from mine tailing. *Int. J. Miner. Process.* 140: 88–94.

Kim, T.W., Ryoo, R., Kruk, M., Gierszal, K.P., Jaroniec,

M., Kamiya, S. and Terasaki, O. (2004). Tailoring the pore structure of SBA-16 silica molecular sieve through the use of copolymer blends and control of synthesis temperature and time. *J. Phys. Chem. B* 108: 11480–11489.

Kosuge, K., Kubo, S., Kikukawa, N. and Takemori, M. (2007). Effect of pore structure in mesoporous silicas on VOC dynamic adsorption/desorption performance. *Langmuir* 23: 3095–3102.

Kubo, S. and Kosuge, K. (2007). Salt-Induced formation of uniform fiberlike SBA-15 mesoporous silica particles and application to toluene adsorption. *Langmuir* 23: 11761–11768.

Langmuir, I. (1916). The constitution and fundamental properties of solids and liquids. Part I. solids. *J. Am. Chem. Soc.* 38: 2221–2295.

Langmuir, I. (1918). The adsorption of gases on plane surface of glass, mica and platinum. *J. Am. Chem. Soc.* 40: 1361–1403.

Lee, D.G., Kim, J.H. and Lee, C.H. (2011). Adsorption and thermal regeneration of acetone and toluene vapors in dealuminated Y-zeolite bed. *Sep. Purif. Technol*. 77: 312–324.

Lee, M.G., Lee, S.W. and Lee, S.H. (2006). Comparison of vapor adsorption characteristics of acetone and toluene based on polarity in activated carbon fixed-bed reactor. *Korean J. Chem. Eng.* 23: 773–778.

Li, L., Sun, Z., Li, H. and, Keener, T.C. (2012). Effects of activated carbon surface properties on the adsorption of volatile organic compounds. *J. Air Waste Manage. Assoc.* 62: 1196–1202.

Li, L., Sun, T.H., Shu, C.H. and Zhang, H.B. (2016). Low temperature H_2S removal with 3-D structural mesoporous molecular sieves supported ZnO from gas stream. *J. Hazard. Mater.* 311: 142–150.

Lin, Y.C., Bai, H. and Chang, C.L. (2005). Applying hexagonal nanostructured zeolite particles for acetone removal. *J. Air Waste Manage. Assoc.* 55: 834–840.

Lin, Y.C. and Bai, H. (2006). Temperature effect on pore structure of nanostructured zeolite particles synthesized by aerosol spray method. *Aerosol Air Qual. Res.* 6: 43–53.

Liu, Y., Li, Z., Yang, X., Xing, Y., Tsai, C., Yang, Q., Wang, Z. and Yang, R.T. (2016). Performance of mesoporous silicas (MCM-41 and SBA-15) and carbon (CMK-3) in the removal of gas-phase naphthalene: adsorption capacity, rate and regenerability. *RSC Adv.* 6: 21193–21203.

Ma, C.M. and Ruan, R.T. (2013). Adsorption of toluene on mesoporous materials from waste solar panel as silica source. *Appl. Clay Sci*. 80–81: 196–201.

Mangun, C.L., Braatz, R.D., Economy, J. and Hall, A.J. (1999). Fixed Bed adsorption of acetone and ammonia onto oxidized activated carbon fibers. *Ind. Eng. Chem. Res.* 38: 3499–3504.

Meynen, V., Cool, P. and Vansant, E.F. (2009). Verified syntheses of mesoporous materials. *Microporous Mesoporous Mater*. 125: 170–223.

Mohammed, J., Nasri, N.S., Ahmad Zaini, M.A., Hamza, U.D. and Ani, F.N. (2015). Adsorption of benzene and toluene onto KOH activated coconut shell based carbon treated with NH_3. *Int. Biodeterior. Biodegrad.* 102: 245–255.

Ng, E.P., Goh, J.Y., Ling, T.C. and Mukti, R.R. (2013). Eco-friendly synthesis for MCM-41 nanoporous materials using the non-reacted reagents in mother liquor. *Nanoscale Res. Lett.* 8: 1–8.

Niknaddaf, S., Atkinson, J.D., Shariaty, P., Jahandar Lashaki, M., Hashisho, Z., Phillips, J.H., Anderson, J.E. and Nichols, M. (2016). Heel formation during volatile organic compound desorption from activated carbon fiber cloth. *Carbon* 96: 131–138.

Rivera-Muñoz, E.M. and Huirache-Acuña, R. (2010). Sol gel-derived SBA-16 mesoporous material. *Int. J. Mol. Sci.* 11: 3069–3086.

Ruthven, D.M. (1984). *Principles of Adsorption and Adsorption Processes.* John Wiley & Sons, New York.

Sakamoto, Y., Kaneda, M., Terasaki, O., Zhao, D.Y., Kim, J.M., Stucky, G., Shin, H.J. and Ryoo, R. (2000). Direct imaging of the pores and cages of three-dimensional mesoporous materials. *Nature* 408: 449–453.

Serrano, D.P., Calleja, G., Botas, J.A. and Gutierrez, F.J. (2004). Adsorption and hydrophobic properties of mesostructured MCM-41 and SBA-15 materials for volatile organic compound removal. *Ind. Eng. Chem. Res.* 43: 7010–7018.

Tang, L., Li, L., Chen, R., Wang, C., Ma, W. and Ma, X. (2016). Adsorption of acetone and isopropanol on organic acid modified activated carbons. *J. Environ. Chem. Eng.* 4: 2045–2051.

Van Der Voort, P., Benjelloun, M. and Vansant, E.F. (2002). Rationalization of the synthesis of SBA-16: Controlling the micro- and mesoporosity. *J. Phys. Chem. B* 106: 9027–9032.

Wang, J., Fang, L., Cheng, F., Duan, X. and Chen, R. (2013). Hydrothermal synthesis of SBA-15 using sodium silicate derived from coal gangue. *J. Nanomater.* 2013: 1–6.

Wei, J., Shi, J., Pan, H., Zhao, W., Ye, Q. and Shi, Y. (2008). Adsorption of carbon dioxide on organically functionalized SBA-16. *Microporous Mesoporous Mater*. 116: 394–399.

Wu, L., Zhang. L., Meng, T., Yu, F., Chen, J. and Ma, J. (2015). Facile synthesis of 3D amino-functional graphene-sponge composites decorated by graphene nanodots with enhanced removal of indoor formaldehyde. *Aerosol Air Qual. Res.* 15: 1028-1034.

Zhang, W., Qu, Z., Li, X., Wang, Y., Ma, D. and Wu, J. (2012). Comparison of dynamic adsorption/desorption characteristics of toluene on different porous materials. *J. Environ. Sci.* 24: 520–528.

Zhao, D., Feng, J., Huo, Q., Melosh, N., Fredrickson, G.H., Chmelka, B.F. and Stucky, G.D. (1998). Triblock copolymer syntheses of mesoporous silica with periodic 50 to 300 angstrom pores. *Science* 279: 548–552.

Received for review, January 15, 2016
Revised, June 21, 2016
Accepted, August 4, 2016